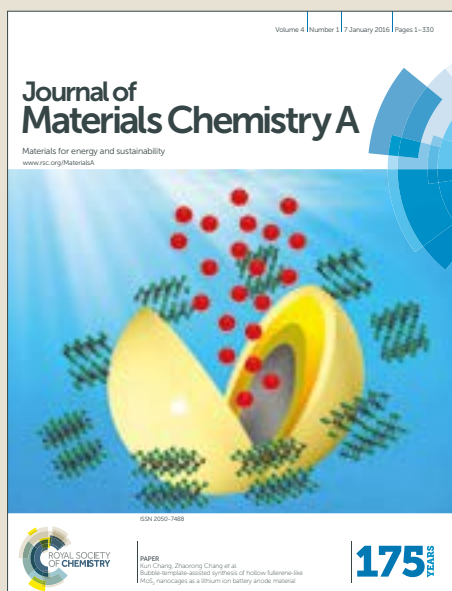


# Journal of Materials Chemistry A

Accepted Manuscript



This article can be cited before page numbers have been issued, to do this please use: S. J. Park, S. H. Jeon, I. K. Lee, J. Zhang, H. Jeong, J. Park, J. Bang, T. K. Ahn, H. Shin, B. G. Kim and H. J. Park, *J. Mater. Chem. A*, 2017, DOI: 10.1039/C7TA02440A.



This is an Accepted Manuscript, which has been through the Royal Society of Chemistry peer review process and has been accepted for publication.

Accepted Manuscripts are published online shortly after acceptance, before technical editing, formatting and proof reading. Using this free service, authors can make their results available to the community, in citable form, before we publish the edited article. We will replace this Accepted Manuscript with the edited and formatted Advance Article as soon as it is available.

You can find more information about Accepted Manuscripts in the [author guidelines](#).

Please note that technical editing may introduce minor changes to the text and/or graphics, which may alter content. The journal's standard [Terms & Conditions](#) and the ethical guidelines, outlined in our [author and reviewer resource centre](#), still apply. In no event shall the Royal Society of Chemistry be held responsible for any errors or omissions in this Accepted Manuscript or any consequences arising from the use of any information it contains.

# Inverse Type Planar Heterojunction Perovskite Solar Cells with Dopant Free Hole Transporting Material: Lewis Base-Assisted Passivation and Charge Recombination

Sang Jin Park,<sup>1,†</sup> Seolhee Jeon,<sup>2,†</sup> In Kyu Lee,<sup>2,†</sup> Jing Zhang,<sup>1</sup> Huiseong Jeong,<sup>1,3</sup> Ji-Yong Park,<sup>1,3</sup> Jiwon Bang,<sup>4</sup> Tae Kyu Ahn,<sup>5</sup> Hee-Won Shin,<sup>5</sup> Bong-Gi Kim<sup>2,\*</sup> and Hui Joon Park<sup>1,6,\*</sup>

<sup>1</sup>Department of Energy Systems Research, Ajou University, Suwon 16499, Republic of Korea

<sup>2</sup>Department of Organic and Nano System Engineering, Konkuk University, Seoul 05029, Republic of Korea

<sup>3</sup>Department of Physics, Ajou University, Suwon 16499, Republic of Korea

<sup>4</sup>Nano convergence Materials Center, Korea Institute of Ceramic Engineering & Technology, Jinju 52851, Republic of Korea

<sup>5</sup>Department of Energy Science, Sungkyunkwan University, Suwon 16419, Republic of Korea

<sup>6</sup>Department of Electrical and Computer Engineering, Ajou University, Suwon 16499, Republic of Korea

\*Corresponding Authors: [huijoon@ajou.ac.kr](mailto:huijoon@ajou.ac.kr), [bgkim2015@konkuk.ac.kr](mailto:bgkim2015@konkuk.ac.kr)

<sup>†</sup>S.J.P., S.J. and I.K.L. contributed equally to this work.

**Keywords:** triarylamine, dopant free hole transporting material, perovskite solar cell, charge recombination, organic electronics

**Abstract:** Three novel triarylamine derivatives (TPACs: TPAC0M, TPAC2M and TPAC3M) sharing the same conjugation scaffold but possessing the different number of methoxy unit, were designed for high performance hole transport materials (HTMs) of perovskite solar cells (PSCs), especially p-i-n inverse-type planar heterojunction PSCs, and synthesized through a simple suzuki-type coupling reaction. From cyclic voltammetry and absorption results, it was shown that their energy levels would be beneficial to work as a HTM of PSCs. In addition, time-resolved photoluminescence measurement and transient photo-voltage study proved that TPACs-based PSCs had better charge extraction and more suppressed non-radiative recombination properties than PEDOT:PSS-based PSCs, leading to superior power conversion efficiency (PCE). Furthermore, we confirmed that the applied methoxy units to the triarylamine derivatives did not cause noticeable changes on their optical properties, such as absorption and bandgap, electrical conductance, measured by conductive atomic force microscopy, and mobility, but the charge extraction and recombination behaviors of TPACs-based PSCs could be improved by increasing the numbers of methoxy unit in arylamine moiety, expected to act as Lewis base that could passivate the defect sites at the interface between HTM and perovskite, analyzed by X-ray photoelectron spectroscopy depth measurement, consequently resulting in an increase of their PCE to 17.54 % without any dopants.

View Article Online  
DOI: 10.1039/C7TA02440A

## Introduction

Organic semiconductors have been intensively investigated, as a potential candidate, to replace inorganic semiconductor or conductor, because of their unlimited modification ability and intrinsically flexible characteristic. Especially, exhaustive explorations on the charge transfer mechanism in organic semiconductors have enlarged their possible application areas, such as organic light emitting diode (OLED),<sup>1</sup> photovoltaic (PV) device<sup>2</sup> and field-effect transistor (FET).<sup>3</sup> Recently, organic-inorganic hybrid perovskite solar cells (PSCs), which utilized a perovskite material as photoactive layer, have drawn great attention because of relatively higher power conversion efficiency (PCE), compared to the PV devices adopting an organic semiconductor as active layer.<sup>4</sup> Perovskites are efficient light harvesting materials with bipolar transport property and long carrier diffusion length, but it has been shown that organic semiconductor-based hole transport materials (HTMs), which extract holes from the perovskite layer and transport them to an electrode, could play a crucial role for high efficiency PSCs.<sup>5</sup> In order to achieve higher light-to-electrical energy conversion efficiency in PSCs, the organic HTMs should have an appropriate energy level alignment with perovskites and a good charge carrier mobility to minimize both electrical potential loss and charge recombination. For this purpose, organic semiconductors having strong crystallization behaviour<sup>6</sup> or versatile feasibility of chemical doping<sup>7</sup> were dominantly considered as effective HTMs in PSC, because of their superior electrical mobility in comparison with amorphous organic semiconductors.

In OLEDs, triarylamine derivatives are predominantly considered as HTMs, because the amine atom is relatively easy to lose one electron and the resulting radical cation, potential hazard for long-term stability of electronic devices, can be stabilized by resonance effect of adjacent aryl substituents.<sup>8</sup> However, the inherently low electrical mobility of the triarylamine derivative, due to amorphous-like characteristics, has restricted their broad application to

PSCs, unless they were chemically doped to improve the electrical charge mobility.<sup>9</sup> Since the chemical doping would cause potential issues, such as high cost, complicate fabrication and dopant-induced device degradation,<sup>10</sup> devising highly efficient dopant-free HTM is one of inevitable demands to make further advancement of PSCs.

Meanwhile, most recent PSCs have either n-i-p-type or p-i-n-type configurations. Even though the highest efficiencies over 20% PCE have been reported from n-i-p-type configuration PVs, built on thick mesoporous (mp) metal-oxide scaffold, their complicated preparation procedures and needs for high temperature annealing hampered the extension of PSC technology to low-cost flexible devices that can be fabricated by a high-speed roll-to-roll process.<sup>4</sup> Moreover, without the mp metal-oxide layer, n-i-p-type PSCs often have severe hysteretic behavior. Therefore, the necessity of high performance HTM, which can realize p-i-n type planar heterojunction (HJ) PSCs by simple one-step solution-process at low temperature as well as those with long-term stability is continuously increasing.

In this contribution, three triarylamine derivatives were newly synthesized and their optical and electrical properties were evaluated as HTMs of p-i-n inverse-type planar HJ PSCs. When they were adopted as HTMs in this configuration, overall power conversion efficiency (PCE) reached over 17% without any chemical doping treatment. When the optical and electrical properties of the synthesized triarylamine derivatives were explored, it was shown that the Lewis-base effect of the methoxy group at the triarylamine derivative backbone, analyzed by X-ray photoelectron spectroscopy (XPS) depth measurement, played an important role to increase charge extraction property and to reduce charge recombination, ultimately resulting in better device performances including the enhancement of short circuit current ( $J_{sc}$ ) and open circuit voltage ( $V_{oc}$ ). In addition, the structure dependent charge extraction and recombination tendencies were systematically correlated by both time-resolved photoluminescence (TRPL) and transient photo-voltage (TPV) studies.

## Results and discussion

View Article Online  
DOI: 10.1039/C7TA02440A

As illustrated in Fig. 1 and Scheme S1, we designed and synthesized three novel triarylamine derivatives (TPACs: TPAC0M, TPAC2M and TPAC3M) sharing a same conjugated backbone to which the different numbers of methoxy unit attached. All triarylamine derivatives were obtained from one- or a two-step simple chemical reaction, and their structures were fully characterized by means of  $^1\text{H-NMR}$  and mass spectroscopy. When the absorption characteristics of the obtained TPACs were compared, they showed nearly same absorption spectra both in solution and film state (Fig. S1), reflecting an amorphous-like physical nature which is commonly shown in triarylamine derivatives.<sup>11</sup> Introduction of electron donating methoxy groups to the triarylamine (TPAC2M) or carbazole (TPAC3M) moieties caused absorption red-shift slightly (15 nm) or little change, respectively. However, the introduced methoxy groups noticeably changed the molecular energy levels in the TPACs. The highest occupied molecular orbital (HOMO) energy levels of TPACs were directly measured by means of cyclic voltammetry (CV) and the lowest unoccupied molecular orbital (LUMO) energy levels were estimated with their absorption onset. As shown in Fig. S2 and Fig. 1b, TPAC2M containing two methoxy units at the diphenylamine moiety exhibited relatively shallow HOMO level, rather than TPAC0M having no methoxy unit. The additional introduction of the electron donating methoxy group to the phenyl carbazole moiety did not significantly change molecular energy levels, including optical band-gap (TPAC3M). Based on the obtained energy levels, we could speculate that TPACs have enough potential to function as efficient HTMs in PSC, because their shallow HOMO levels, compared to that (-5.4 eV) of perovskite, would be beneficial to extract hole from perovskite layer and the shallow LUMO levels would effectively block electron transfer from perovskite layer to HTM, respectively.<sup>12</sup>

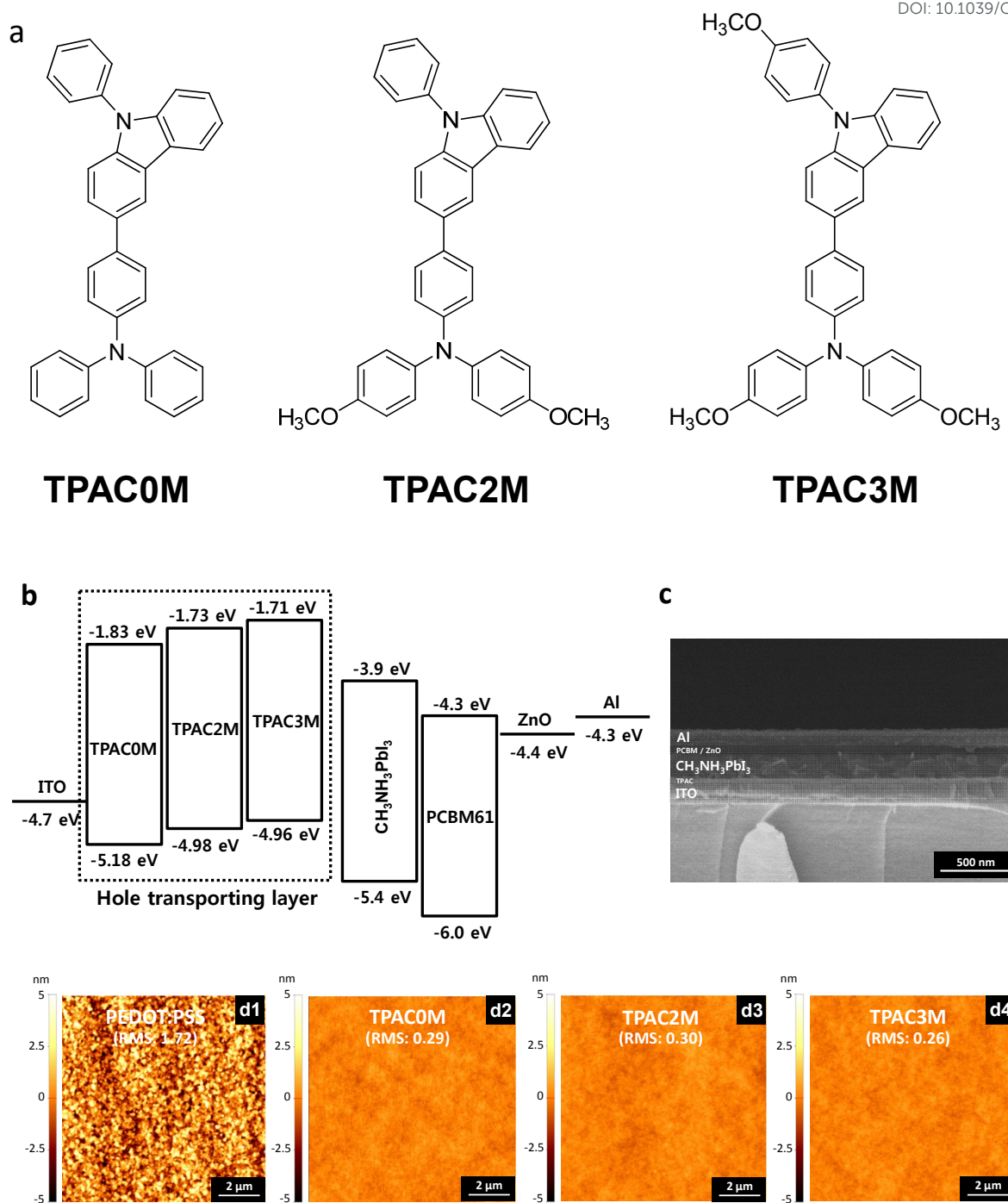


**Fig. 1.** a) Detailed chemical structures of obtained novel triarylamine derivatives for dopant free hole transporting materials. b) Energy level of each layer of perovskite solar cell. c) Cross-sectional SEM of TPACs-based perovskite solar cell (TPAC3M-based device as a representative). AFM height images of d1) PEDOT:PSS, d2) TPAC0M, d3) TPAC2M, and d4) TPAC3M on ITO electrode. RMS values of PEDOT:PSS, TPAC0M, TPAC2M, and TPAC3M on ITO are 1.72, 0.29, 0.30, and 0.26 nm, respectively.

To investigate the performances of TPACs as dopant free HTMs, we fabricated p-i-n inverse type planar HJ PSCs as following configuration: ITO / HTM / CH<sub>3</sub>NH<sub>3</sub>PbI<sub>3</sub> / [6,6]-phenyl-C<sub>61</sub>-butyric acid methyl ester (PCBM) / ZnO / Al. Additionally, PEDOT:PSS, one of the most widely utilized organic conductors, was also applied as a HTM to relatively compare the charge extraction and transfer efficiency in PSCs. Atomic force microscopy (AFM) topological images of HTMs in Fig. 1d confirmed that the height variation of the surface of TPACs on ITO was within a nanometer, of which the root mean square (RMS) roughness was around 0.3 nm, much lower than that of PEDOT:PSS (1.7 nm). Therefore, TPACs could more efficiently planarize the rough ITO surface than PEDOT:PSS, and it is expected that their uniformity would not induce any morphological difference in the following perovskite photoactive layer. The optimized film formation condition of TPACs was 20 mg/ml at 1000 rpm (Table S1), giving the thickness in the range of 40 nm – 50 nm (Fig. 1c). In Fig. 2a and Table 1, the performances of PSCs, which utilized newly obtained TPACs and PEDOT:PSS as HTMs, are summarized. All TPACs-based PSCs exhibited better device performances than the PEDOT:PSS-based PSCs, and in particular, PSCs with TPAC3M showed the best performance over 17% of PCE without any chemical doping treatment. TPACs-based PSCs also showed better stability than PEDOT:PSS-based PSCs (Fig. S3). All *J-V* characteristics of our PSCs showed negligible hysteresis depending on scan directions, indicating stable operation of each cell (Fig. S4).

**Table 1.** Summary of device performance of perovskite solar cell adopting different hole transporting materials

HTM Materials	V <sub>oc</sub> (V)	J <sub>sc</sub> (mA/cm <sup>2</sup> )	FF	PCE (%)
PEDOT:PSS	0.86 (0.87)	18.23 (18.57)	0.73 (0.78)	11.44 (12.60)
TPAC0M	0.92 (0.91)	19.80 (20.73)	0.72 (0.74)	12.92 (13.92)
TPAC2M	0.98 (0.99)	21.68 (22.58)	0.72 (0.71)	15.20 (15.77)
TPAC3M	0.99 (1.00)	22.11 (22.79)	0.75 (0.78)	16.58 (17.54)

Numbers are average values of forward and reverse scan data, measured from over 30 devices for each condition (values in parentheses are from the best performing devices).

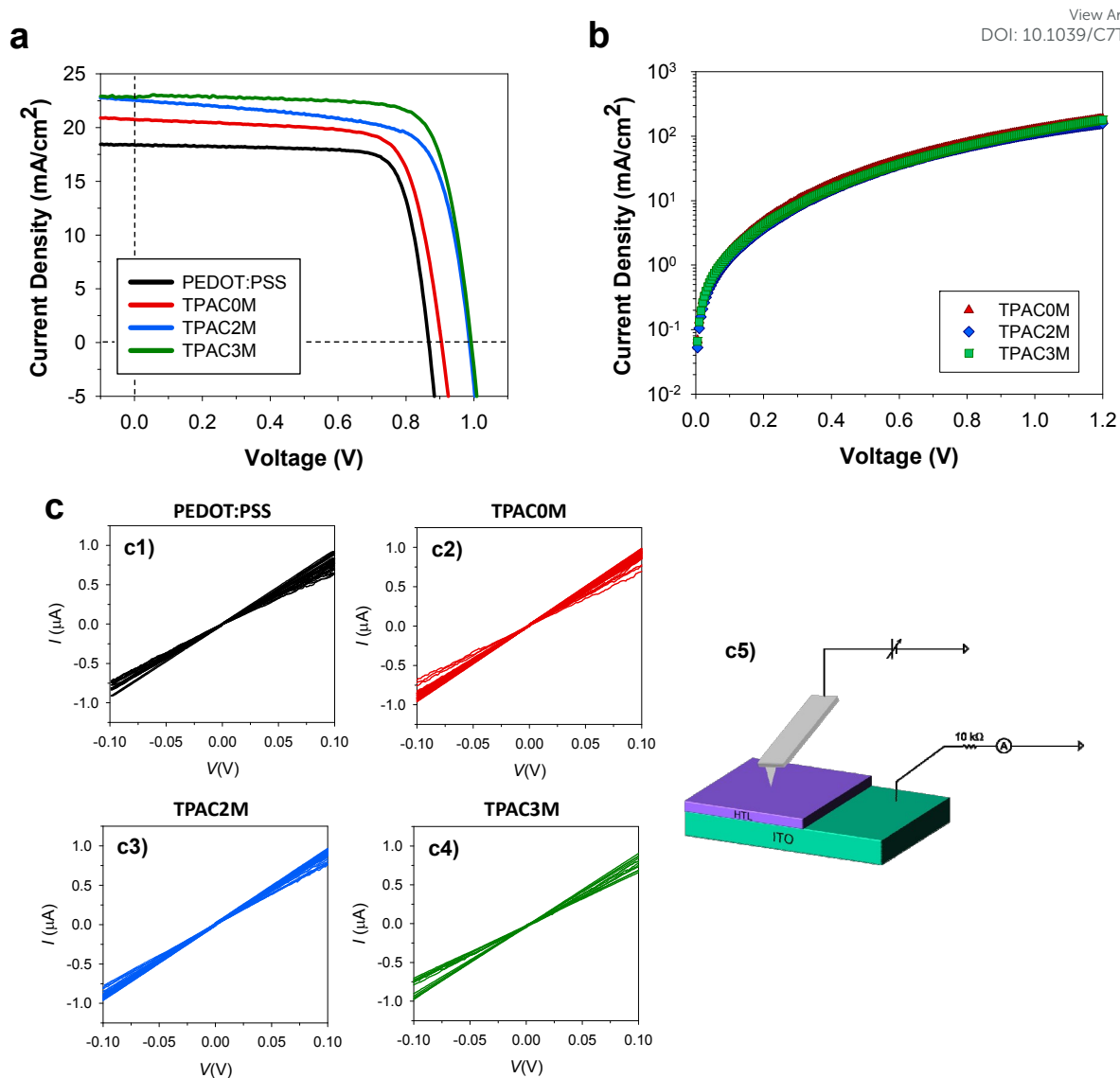


**Fig. 2.** a)  $J$ - $V$  curves of PEDOT:PSS- and TPACs (TPAC0M, TPAC2M, and TPAC3M)-based perovskite solar cells. All data were measured at AM 1.5 G ( $100 \text{ mW}\cdot\text{cm}^{-2}$  intensity). b) Measured  $\log J$ - $V$  plots under dark conditions for hole-only devices. The calculated hole mobility values of TPAC0M, TPAC2M, and TPAC3M from the SCLC method are  $1.2 \times 10^{-5}$ ,  $1.0 \times 10^{-5}$ ,  $1.1 \times 10^{-5} \text{ cm}^2\text{V}^{-1}\text{s}^{-1}$ , respectively. c)  $I$ - $V$  curves of c1) PEDOT:PSS, c2) TPAC0M, c3) TPAC2M and c4) TPAC3M measured by c-AFM. The mean values of resistances (standard deviations), measured from PEDOT:PSS, TPAC0M, TPAC2M, and TPAC3M by c-AFM, are 2.1 (0.9), 1.1 (0.6), 1.1 (0.6), and 1.5 (0.8)  $\text{k}\Omega$ , respectively. c5) Schematic diagram of c-AFM measurement.

The enhanced  $J_{sc}$  of TPACs-based PSCs could be originated from the better charge transfer efficiency in HTM or/and the effective charge extraction from the perovskite layer.

Since both PEDOT:PSS and TPACs have negligible optical density on the high photon flux region, the most amounts of photocurrent could be generated from the applied perovskite photo-absorber after absorption of same amount solar light. In order to evaluate the charge transfer efficiency in HTM, we measured electrical conductivity of HTM in vertical direction by conductive atomic force microscopy (c-AFM), as shown in Fig. 2c. Interestingly, resistances measured from all HTMs showed almost similar level (1~2 k $\Omega$ ) and their variation was within standard deviation, suggesting that charge transport behavior may be not be a crucial factor to explain the improved photocurrent generation of TPACs. This was further confirmed by mobility values in vertical direction measured by hole-only devices, which utilized high work-function molybdenum oxide (MoO<sub>3</sub>) instead of ZnO to block the injection of electrons from the Al cathode, using the space-charge-limited current (SCLCs) method at low voltage:  $J = 9\epsilon_0\epsilon_r\mu V^2/8L^3$ , where  $\epsilon_0\epsilon_r$  is the permittivity of the component,  $\mu$  is the carrier mobility, and  $L$  is the thickness.<sup>13</sup> As shown in Fig. 2b, the measured hole mobilities from PSCs with TPACs were similar (TPAC0M =  $1.2\times 10^{-5}$  cm<sup>2</sup>·V<sup>-1</sup>·s<sup>-1</sup>, TPAC2M =  $1.0\times 10^{-5}$  cm<sup>2</sup>·V<sup>-1</sup>·s<sup>-1</sup>, and TPAC3M =  $1.1\times 10^{-5}$  cm<sup>2</sup>·V<sup>-1</sup>·s<sup>-1</sup>).

To examine the charge extraction ability of doping-free TPACs from perovskite photoactive layer as HTM, we prepared Quartz(Q)/doping-free TPACs (TPAC0M, TPAC2M or TPAC3M)/CH<sub>3</sub>NH<sub>3</sub>PbI<sub>3</sub> samples and measured their PL lifetimes by time-correlated single photon counting (TCSPC), maintaining Q/PEDOT:PSS/CH<sub>3</sub>NH<sub>3</sub>PbI<sub>3</sub> as a reference to TPACs. The PL decay curves of each sample were convoluted using bi-exponential functions and were plotted in Fig. 3a. The Q/PEDOT:PSS/CH<sub>3</sub>NH<sub>3</sub>PbI<sub>3</sub> showed an averaged PL lifetime ( $\tau_{ave}$ ) of 7.34 ns; a fast decay component,  $\tau_1$ , of about 2.1 ns and slow decay component,  $\tau_2$ , of 12.1 ns. Those PL lifetimes were shortened with applying a HTM to TPACs-based samples. Especially, TPAC3M with three electron-donating methoxy units showed the shortest PL lifetime of  $\tau_{ave}$ =3.68 ns, compared to those ( $\tau_{ave}$ =4.27 ns,  $\tau_{ave}$ =4.98 ns) of TPAC2M with two

methoxy units and TPAC0M without functional groups, respectively, indicating that TPAC3M has about a twofold increase in charge extraction rate compared to that of PEDOT:PSS, which is advantageous to get better photocurrent generation. The detailed information about bi-exponential fitting result is in Table S2. This photogeneration trend is well-matched with  $J_{sc}$  values of TPACs- and PEDOT:PSS-based PSCs; TPAC3M: 22.79 mA/cm<sup>2</sup> > TPAC2M: 22.58 mA/cm<sup>2</sup> > TPAC0M: 20.73 mA/cm<sup>2</sup> > PEDOT:PSS: 18.57 mA/cm<sup>2</sup>. The EQE signals of PSCs with TPAC3M and PEDOT:PSS are in Fig. S5. From the PL decays and  $J_{sc}$  result, we could also conclude that the electron-donating methoxy units attached to triarylamine (TPAC2M) or carbazole (TPAC3M) moieties could play a crucial role to improve the device performances, which will be discussed in detail.

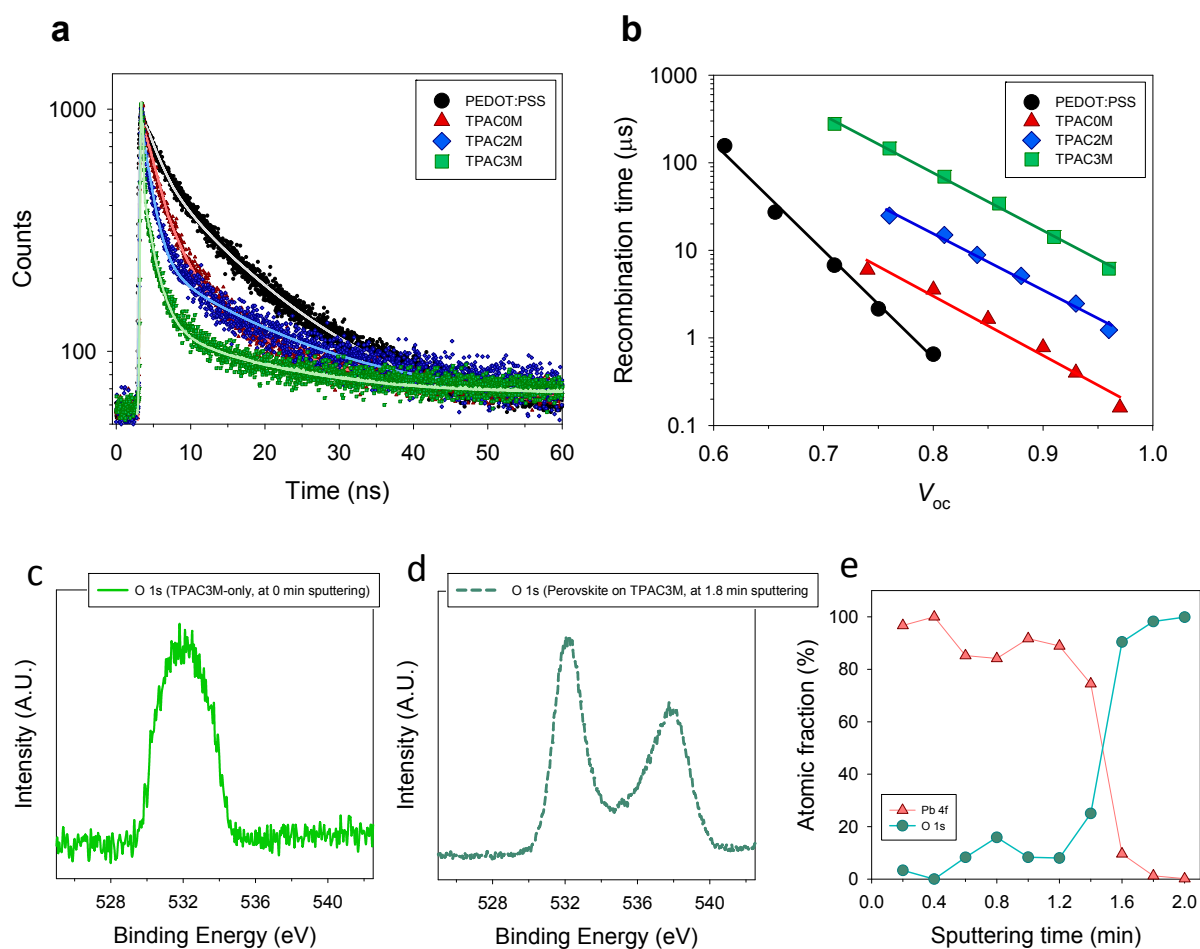


**Fig. 3.** a) PL decay curves of perovskite/HTM layers on quartz at peak emission wavelength (770 nm), excited with 670 nm from quartz side. Black, red, blue and green colors represent PEDOT:PSS, TPAC0M, TPAC2M and TPAC3M. b) Recombination lifetime vs.  $V_{oc}$  plots of complete cells having PEDOT:PSS (black), TPAC0M (red), TPAC2M (blue) and TPAC3M (green) as a HTM, which measured by transient photovoltage (TPV) experiment. XPS spectra showing the O 1s region of (c) TPAC3M-only sample at 0 min sputtering and (d) perovskite-casted TPAC3M sample at 1.8 min sputtering. e) XPS depth profiles of perovskite-casted TPAC3M sample.

In addition to  $J_{sc}$ , we explored the recombination behavior of photo-carriers in PSC devices using TPV measurement to clarify the  $V_{oc}$  variation among devices. As we have shown in Fig. 2a and Table 1, all TPACs-based PSCs showed superior  $V_{oc}$  to PEDOT:PSS-based PSCs, even though HOMO levels of TPAC-series are comparable (TPAC0M = 5.18 eV) to or even lower (TPAC2M = 4.98 eV, TPAC3M = 4.96 eV) than that of PEDOT:PSS (known to be about 5.2 eV). Moreover, TPAC3M having the lowest HOMO level due to the electron donating methoxy units in its conjugated backbone, produced higher  $V_{oc}$  than that of TPAC0M without any methoxy unit in the same conjugated backbone. The  $V_{oc}$  values of the devices are 1.00 V > 0.99 V > 0.91 V > 0.87 V for TPAC3M, TPAC2M, TPAC0M, PEDOT:PSS, respectively. Therefore, we speculated that the recombination behavior of photo-carrier in those PSC structures, which directly influenced their  $V_{oc}$ , would be different between TPACs and PEDOT:PSS and that it could be further manipulated by changing the number of electron donating methoxy units, attached to their conjugated backbone. To investigate the charge recombination behavior in actual device structures, we used the TPV measurement.<sup>14</sup> Fig. 3b shows the averaged charge recombination lifetimes ( $\tau_n$ ) from three types of TPACs- and PEDOT:PSS-based PSCs, measured with an increment in  $V_{oc}$ . PSCs with doping-free TPACs as HTMs revealed much longer  $\tau_n$  than that of PEDOT:PSS as a HTM in the entire range of  $V_{oc}$ . Furthermore, the more methoxy units TPAC conjugated backbone has, the longer  $\tau_n$  TPAC-based PSCs have. The longer  $\tau_n$  would be beneficial to

reduce recombination event and to increase the possibility of charge extraction in actual device structures. Consequently, the longer  $\tau_n$  provided better performances of devices including  $V_{oc}$ . The change of recombination behavior in device structure in an accord with the utilized HTMs is well-matched with their  $V_{oc}$  variation.

The aforementioned changes in kinetics of excitons and free carriers depending on kinds of HTMs suggest that trap density at the interface between HTM and perovskite could be reduced by introducing methoxy units to TPACs. It has been reported that Lewis bases such as thiophene, pyridine and methoxy group could passivate defect sites such as under-coordinated Pb atoms on the crystal surface and at the grain boundaries, often generated during the annealing process of perovskites, resulting in decreasing non-radiative recombination in perovskite films.<sup>15</sup> In order to clarify if methoxy group at TPAC2M and TPAC3M worked as Lewis base at the interface between TPACs HTM and perovskite, XPS depth analysis was performed to directly investigate the interfacial chemical states. Fig. 3c and d show XPS spectra showing the O 1s regions of the TPAC3M-only sample and perovskite-casted TPAC3M sample. As for the signal of perovskite-casted TPAC3M sample, the perovskite/TPAC3M interface reference point (around 1.4 ~ 1.6 min of sputtering time), in which the high Pb 4f fraction of perovskite layer significantly decreased (Fig. 3e), was firstly clarified, and the O 1s signal at 1.8 min of sputtering time was utilized for the comparison with that of bare TPAC3M sample. As shown in XPS spectra, higher binding energy O 1s feature (around 538 eV), indicative of a direct interaction of oxygen sites as Lewis base with possible defect sites such as halide vacancy of perovskite,<sup>16</sup> was clearly observed. Although TPACs contain amine showing stronger Lewis basicity than oxygen of methoxy unit, the amine atom of the triarylamine moiety is concealed by the peripheral three phenyl units. Thus, methoxy units attaching to the end of molecule could have higher chance to react with the defect site of perovskite layer. This methoxy group effect was obvious when charge extraction and recombination behaviors of PSCs with three types of TPACs having

different number of methoxy unit were compared, as we showed earlier. As the number of introduced methoxy unit increases from TPAC0M to TPAC3M, charge extraction could be enhanced and recombination be effectively suppressed, which provides higher  $J_{sc}$  and  $V_{oc}$  to PSCs.

View Article Online  
DOI: 10.1039/C7TA02440A

## Conclusions

In summary, we designed and synthesized three novel triarylamine derivatives, which can control carrier extraction and recombination behaviors in PSCs as a high performance HTM by changing the number of electron donating methoxy unit, even without any dopants. As increasing the numbers of methoxy unit in arylamine moiety, expected to act as Lewis base that could passivate the defect sites at the interface between HTM and perovskite, we confirmed that charge extraction from perovskite to HTM was improved and recombination in PSC device was suppressed, increasing their  $J_{sc}$  and  $V_{oc}$ . Consequently, the PCEs of p-i-n inverse type PSCs adopting TPACs as dopant-free HTMs gradually improved from TPAC0M (13.92%) having no methoxy unit to TPAC3M (17.54%) containing three methoxy groups in arylamine moiety.

## Experimental

### Synthesis

All starting materials were purchased from commercial suppliers (Aldrich and TCI). Detailed synthetic procedures are summarized in supporting information and synthesized compounds were fully characterized with  $^1\text{H-NMR}$ ,  $^{13}\text{C-NMR}$ , mass and elemental analysis. (Fig. S6-S14). In addition, the thermal transition and degradation behaviors of final compounds (TPAC0M, TPAC2M and TPAC3M) were characterized with differential scanning calorimetry and thermal gravimetric analysis (Fig. S15), respectively.

**TPAC0M**View Article Online  
DOI: 10.1039/C7TA02440A

Under inert condition, 9-phenylcarbazole-3-boronic Acid (2g, 6.97mmol), 4-bromotriphenylamine (2.052g, 6.33mmol) and Pd(0) (0.374g, 0.32mmol) were placed into round bottom flask. After adding tetrahydrofuran and 2M of K<sub>2</sub>CO<sub>3</sub> solution (48mL/16mL, 3:1 ratio), the mixture was vigorously stirred at 60 °C for 8 hours. Then, the mixture was cooled down to room temperature and quenched by adding deionized water. After extraction with methylene chloride, the organic layer was collected and dried with MgSO<sub>4</sub>. The residual solid was removed by filtration and the solution was evaporated under vacuo. Final compound, TPAC0M, was collected through column chromatography (MC/n-Hexane: 1:3) and consequent recrystallization under MC/n-Hexane mixture, in yield 75%. In order to improve purity, the obtained product was sublimed and used for device fabrication. <sup>1</sup>H-NMR (400MHz, Acetone) δ 8.65 (s, 1H), 8.45 (d, 1H), 7.89-7.82 (m, 5H), 7.80 (d, 2H), 7.69 (t, 1H), 7.63-7.52 (m, 3H), 7.50-7.41 (m, 5H), 7.28 (d, 2H), 7.24 (d, 4H), 7.19 (t, 2H); <sup>13</sup>C NMR (CDCl<sub>3</sub>, 150 MHz, ppm) 147.87, 146.56, 141.35, 140.18, 137.73, 136.32, 133.04, 129.93, 129.29, 127.99, 127.50, 127.09, 126.12, 125.19, 124.47, 124.24, 123.91, 123.53, 122.75, 120.37, 120.06, 118.36, 110.03, 109.94; m/z LC/MS 486.62 and anal. calcd. for C<sub>36</sub>H<sub>26</sub>N<sub>2</sub>: C, 88.86; H, 5.39; N, 5.76; found: C, 88.74; H, 5.40; N, 5.86.

**TPAC2M**

Final product was similarly obtained with the synthetic procedure TPAC0M. 9-Phenylcarbazole-3-boronic Acid (2.052g, 7.15mmol), 4-Bromo-4',4''-dimethoxytriphenylamine (2.5g, 6.51mmol) and Pd(0) (0.385g, 0.33mmol) were used to obtain TPAC2M. <sup>1</sup>H-NMR (400MHz, Acetone) δ 8.59 (s, 1H), 8.43 (d, 1H), 7.89-7.66 (m, 8H), 7.55 (t, 3H), 7.43 (t, 1H), 7.21 (d, 4H), 7.11 (d, 2H), 7.06 (d, 4H), 3.93 (s, 6H); <sup>13</sup>C NMR (CDCl<sub>3</sub>, 150 MHz, ppm) 141.32, 140.03, 137.77, 129.92, 127.46, 127.07, 126.41, 126.07, 125.11, 123.89, 123.56, 120.37, 120.01, 118.15, 114.73, 109.98, 109.90, 55.54; m/z LC/MS 546.67 and anal. calcd.

for  $C_{38}H_{30}N_2O_2$ : C, 83.49; H, 5.53; N, 5.12; O, 5.85; found: C, 83.50; H, 5.51; N, 5.13; O, 5.86.

### TPAC3M

Final product was similarly obtained with the synthetic procedure TPAC0M. 9-(4-methoxyphenyl)-carbazole-3-boronic ester (2.00g, 5.01mmol), 4-Bromo-4',4''-dimethoxy-triphenylamine (1.748g, 4.50mmol) and Pd(0) (0.268g, 0.23mmol) were used to obtain TPAC3M.  $^1H$ -NMR (400MHz, Acetone)  $\delta$  8.58 (s, 1H), 8.41 (d, 1H), 7.80 (d, 1H), 7.74 (d, 2H), 7.67 (d, 2H), 7.58-7.33 (m, 6H), 7.21 (d, 4H), 7.11 (d, 2H), 7.05 (d, 4H), 4.01 (s, 3H), 3.92 (s, 6H);  $^{13}C$  NMR ( $CDCl_3$ , 150 MHz, ppm) 158.89, 155.75, 147.50, 141.81, 141.22, 140.52, 134.39, 133.05, 130.36, 128.51, 127.75, 126.40, 126.01, 125.07, 123.66, 123.32, 121.43, 120.34, 119.77, 118.13, 115.12, 114.74, 109.92, 109.85, 55.63, 55.54; m/z LC/MS 576.70 and anal. calcd. for  $C_{39}H_{32}N_2O_3$ : C, 81.23; H, 5.59; N, 4.86; O, 8.32; found: C, 81.25; H, 5.56; N, 4.88; O, 8.31.

### Cyclic voltammetry measurement

Ag/AgNO<sub>3</sub> served as the pseudo reference electrode, ferrocene was used for calibration, and the supporting electrolyte was tetrabutylammonium hexafluorophosphate (TBAHFP) in acetonitrile (0.1 M). Oxidation and reduction potential of each TPAC series were directly measured under the scan rate of 100 mV/s, after preparation of solution in dichloromethan (1.0 mM).

### Device fabrication

Acetone, isopropyl alcohol (IPA), and deionized (DI) water were sequentially used to clean the patterned ITO-coated glass substrates via ultrasonication. The ITO substrates were treated with oxygen plasma for 5 min before use to improve the wettability of following solution. For PEDOT:PSS HTM, Clevios PVP AI 4083 was deposited on the ITO substrate by spin-casting at 3000 rpm for 30 s and annealed using a hot plate at 150 °C for 20 min. For TPACs-based

perovskite solar cells (PSCs), TPAC0M, TPAC2M or TPAC3M layer was formed on the ITO substrate by spin-casting their solution (1:1 chlorobenzene and acetonitrile mixed solvent, 20 mg/ml concentration) at 1000 rpm for 30 s instead of PEDOT:PSS. After forming a hole transport layer (HTL) on the ITO substrate, the samples were transferred to a N<sub>2</sub> box. CH<sub>3</sub>NH<sub>3</sub>PbI<sub>3</sub> perovskite solution was prepared by dissolving PbI<sub>2</sub> (Sigma Aldrich) and CH<sub>3</sub>NH<sub>3</sub>I (1:1 molar ratio), synthesized following the literature,<sup>4</sup> in the solvent mixture of  $\gamma$ -butyrolactone (GBL) and dimethylsulfoxide (DMSO) (7:3 v/v) for a total concentration of 1.1 M in a N<sub>2</sub> atmosphere. The solution was stirred at 70 °C for at least 12 h before being used. Then, spin-casting the solution along with toluene drop-casting achieved a uniform perovskite layer.<sup>4a</sup> PCBM (20 mg/ml in chlorobenzene) was then spin-cast on top of the perovskite layer and ZnO layer was added by spin-casting ZnO NP solution (Sigma Aldrich) on PCBM as an electron transport layer (ETL). Those perovskite photoabsorber, PCBM and ZnO layers were prepared in a N<sub>2</sub> box. Finally, the samples were transferred into a thermal evaporator and Al (80 nm) was thermally deposited at a base pressure of  $4 \times 10^{-6}$  torr. Over 30 devices were prepared for each process condition. As for hole-only devices for hole mobility calculation, 30 nm MoO<sub>3</sub> was thermally deposited on TPACs without shadow mask instead of ZnO, and Al deposition through the shadow mask completed device fabrication with the following configuration: transparent substrate/ITO/PEDOT:PSS/TPACs/MoO<sub>3</sub>/Al.

### Device characterization

A solar simulator (PEC-L01, Peccell Technologies, Inc.) with an AM 1.5G filter was used to provide 100 mW·cm<sup>-2</sup> of illumination on the PV cells, with the intensity calibrated using a Si photodiode, equipped with an infrared cut-off filter (KG5) to reduce spectral mismatch. *J-V* characteristics were obtained using an Ivium technology Ivium compactstat by scanning the *J-V* curves at a 0.05 V·s<sup>-1</sup> scan rate. UV–visible absorption spectra were recorded with a Jasco V760 UV-Vis NIR spectrophotometer in the 400-850-nm wavelength range at room

temperature. SEM images were obtained by Hitachi S-4800. TRPL curves were recorded using a commercial TCSPC system (FluoTime 200, PicoQuant). Samples were excited by picosecond diode laser of 670 nm (LDH-P-C-670, PicoQuant) with a repetition rate of (4MHz). The emitted PL was collected by a fast photomultiplier tube (PMT) detector (PMA 182, PicoQuant) with a magic angle ( $54.7^\circ$ ) arrangement. The incident angle of excitation pulse was set to be about  $30^\circ$  with respect to the sample. The resulting instrumental response function was about 160 ps in full-width-half-maximum. And the PL decays were measured at the emission peak ( $770\pm 5\text{nm}$ ) for perovskite. In addition, a cut-off filter (FF01-692nm, Semrock) was applied to block the remaining scattering and the excitation intensity was controlled using a neutral density filter set in order to avoid unwanted nonlinear effects. TPV decay measurement was performed using a nanosecond OPO laser system (INDI-40-10, Spectra-Physics) as a small perturbation light source and a Xe lamp (LS-150-XE ABET) as a bias light source. The devices were directly connected to a digital oscilloscope (DSO-X 3054A, Agilent) and the input impedance was set to be  $1\text{ M}\Omega$  for an open circuit condition. The bias light intensity was controlled by neutral density filters for various  $V_{oc}$  and the generated voltage transient ( $\Delta V$ ) by an attenuated laser pulse of 550 nm did not exceed 20 mV. All the films, utilized to measure absorption, TRPL, and TPV, were the same as those for solar cell devices. To investigate conductivity of HTL, local  $I-V$  measurements were carried out using conventional AFM (XE-100, Park Systems). Platinum-coated AFM tip has  $< 40\text{ nm}$  tip radius for better electrical contact, and force constant is  $2.7\text{ N/m}$  to avoid destruction of HTLs. XPS depth profiling was applied to investigate the buried interface between TPACs and perovskite under the conditions of an Ar ion gun power of 2 kV and 1 mA on a raster area of  $2\times 2\text{ mm}$ , yielding an equivalent sputtering rate of  $10\text{ nm}\cdot\text{min}^{-1}$  of  $\text{SiO}_2$ . All the binding energies of the XPS data were calibrated with reference to the C-C bond in C 1s ( $284.5\text{ eV}$ ).

View Article Online  
DOI: 10.1039/C7TA02440A

## Acknowledgments

View Article Online  
DOI: 10.1039/C7TA02440A

This research was supported by Basic Science Research Program through the National Research Foundation of Korea (NRF) funded by the Ministry of Science, ICT & Future Planning (NRF-2015R1C1A1A02036659) and the Ministry of Education (NRF-2014R1A1A2056403). This research was also supported by the Industrial Fundamental Technology Development Program (10063268) funded by the Ministry of Trade, Industry & Energy (MOTIE) of Korea and by the National Research Council of Science and Technology (NST) through Degree and Research Center (DRC) Program(2015).

## Notes and references

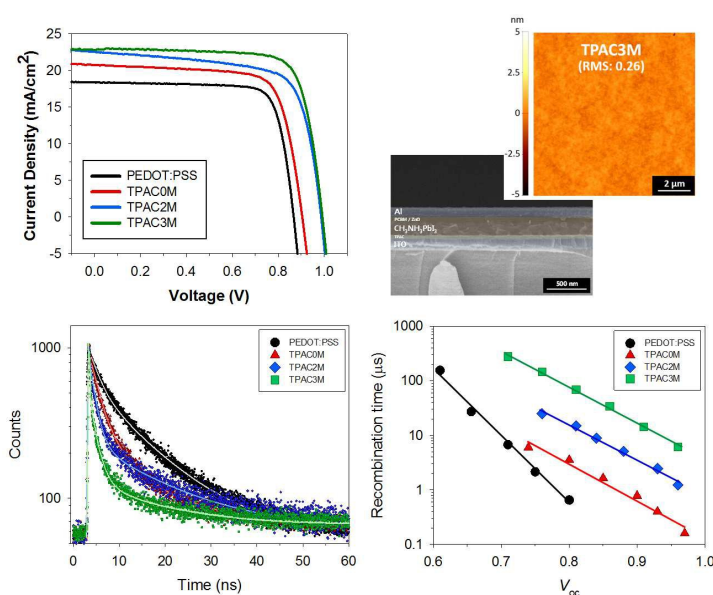
- [1] a) G. Zhou, C. -L. Ho, W. -Y. Wong, Q. Wang, D. Ma, L. Wang, Z. Lin, T. B. Marder, A. Beeby, *Adv. Funct. Mater.*, 2008, **18**, 499; b) A. P. Kulkarni, X. Kong, S. A. Jenekhe, *Adv. Funct. Mater.*, 2006, **16**, 1057; c) S. R. Forrest, *Nature*, 2004, **428**, 911; d) W. Li, Y. Pan, R. Xiao, Q. Peng, S. Zhang, D. Ma, F. Li, F. Shen, Y. Wang, B. Yang, Y. Ma, *Adv. Funct. Mater.*, 2014, **24**, 1609.
- [2] a) C. Deibel, T. Strobel, V. Dyakonov, *Adv. Mater.*, 2010, **22**, 4097; b) S. H. Park, A. Roy, S. Beaupré, S. Cho, N. Coates, J. S. Moon, D. Moses, M. Leclerc, K. Lee, A. J. Heeger, *Nat. Photon.*, 2009, **3**, 297; (c) H. J. Park, J. Y. Lee, T. Lee, L. J. Guo, *Adv. Energy Mater.*, 2013, **3**, 1135; d) D. Veldman, S. C. J. Meskers, R. A. J. Janssen, *Adv. Funct. Mater.*, 2009, **19**, 1939; e) T. M. Clarke, J. R. Durrant, *Chem. Rev.*, 2010, **110**, 6736.; f) Y. Xue, P. Guo, H.-L. Yip, Y. Li, Y. Cao, *J. Mater. Chem. A*, 2017, **5**, 3780.
- [3] a) E. J. Meijer, D. M. de Leeuw, S. Setayesh, E. van Veenendaal, B. -H. Huisman, P. W. M. Blom, J. C. Hummelen, U. Scherf, T. M. Klapwijk, *Nat. Mater.*, 2003, **2**, 678; b) S. Kobayashi, T. Nishikawa, T. Takenobu, S. Mori, T. Shimoda, T. Mitani, H. Shimotani, N. Yoshimoto, S. Ogawa, Y. Iwasa, *Nat. Mater.*, 2004, **3**, 317; c) H.

- Bronstein, Z. Chen, R. S. Ashraf, W. Zhang, J. Du, J. R. Durrant, P. S. Tuladhar, K. Song, S. E. Watkins, Y. Geerts, M. M. Wienk, R. A. J. Janssen, T. Anthopoulos, H. Sirringhaus, M. Heeney, I. McCulloch, *J. Am. Chem. Soc.*, 2011, **133**, 3272; d) K. –J. Baeg, Y. –Y. Noh, J. Ghim, B. Lim, D. –Y. Kim, *Adv. Funct. Mater.*, 2008, **18**, 3678.
- [4] a) N. J. Jeon, J. H. Noh, W. S. Yang, Y. C. Kim, S. Ryu, J. Seo, S. I. Seok, *Nature*, 2015, **517**, 476; b) W. Nie, H. Tsai, R. Asadpour, J. –C. Blancon, A. J. Neukirch, G. Gupta, J. J. Crochet, M. Chhowalla, S. Tretiak, M. A. Alam, H. –L. Wang, A. D. Mohite, *Science*, 2015, **347**, 522; c) S. H. Jeon, U. K. Thakur, D. Lee, Y. Wenping, D. Kim, S. Lee, T.-K. Ahn, H. J. Park, B.-G. Kim, *Org. Electron.*, 2016, **37**, 134; d) W. S. Yang, J. H. Noh, N. J. Jeon, Y. C. Kim, S. Ryu, J. Seo, S. I. Seok, *Science*, 2015, **348**, 1234; e) C. –G. Wu, C. –H. Chiang, Z. –L. Tseng, M. K. Nazeeruddin, A. Hagfeldt, M. Grätzel, *Energy Environ. Sci.*, 2015, **8**, 2725; f) H. Zhou, Q. Chen, G. Li, S. Luo, T. Song, H. –S. Duan, Z. Hong, J. You, Y. Liu, Y. Yang, *Science*, 2014, **345**, 542; g) D. Bi, W. Tress, M. I. Dar, P. Gao, J. Luo, C. Renevier, K. Schenk, A. Abate, F. Giordano, J.-P. C. Baena, J.-D. Decoppet, S. M. Zakeeruddin, M. K. Nazeeruddin, M. Grätzel, A. Hagfeldt, *Sci. Adv.*, 2016, **2**, e1501170; h) X. Li, D. Bi, C. Yi, J.-D. Decoppet, J. Luo, S. M. Zakeeruddin, A. Hagfeldt, M. Grätzel, *Science*, 2016, **353**, 58; i) M. Saliba, T. Matsui, K. Domanski, J.-Y. Seo, A. Ummadisingu, S. M. Zakeeruddin, J.-P. Correa-Baena, W. R. Tress, A. Abate, A. Hagfeldt, M. Grätzel, *Science*, 2016, **354**, 206; j) C. Zuo, H. J. Bolink, H. Han, J. Huang, D. Cahen, L. Ding, *Adv. Sci.*, 2016, **3**, 1500324; k) C. Zuo, L. Ding, *Adv. Energy Mater.* 2017, **7**, 1601193; l) C. Zuo, L. Ding, *Small* 2015, **11**, 5528.
- [5] J. W. Lee, D. J. Seo, A. N. Cho, N. G. Park, *Adv. Mater.*, 2014, **26**, 4991; b) J. A. Christians, R. C. M. Rung, P. V. Kamat, *J. Am. Chem. Soc.*, 2014, **136**, 758; c) B. Conings, L. Baeten, C. D. Dobbelaere, J. D’Haen, J. Manca, H. G. Boyen, *Adv. Mater.*, 2014, **26**, 2041; d) U. Kwon, B.-G. Kim, C. D. Nguyne, J.-H. Park, N. Y. Ha, S.-J.

- Kim, S. H. Ko, S. Lee, D. Lee, H. J. Park, *Sci. Rep.*, 2016, **6**, 30759; e) Y. S. Kwon, *Energy Environ. Sci.*, 2014, **7**, 1454; f) O. Malinkiewicz, A. Yella, Y. H. Lee, G. M. Espallargas, M. Grätzel, M. K. Nazeeruddin, H. J. Bolink, *Nat. Photon.*, 2014, **8**, 128; g) Z. Hawash, L. K. Ono, S. R. Raga, M. V. Lee, Y. B. Qi, *Chem. Mater.*, 2015, **27**, 562.
- [6] a) H. Li, K. Fu, A. Hagfeldt, M. Grätzel, S. G. Mhaisalkar, A. C. Grimsdale, *Angew. Chem. Int. Ed.*, 2014, **53**, 4085; b) G. -W. Kim, G. Kang, J. Kim, G. -Y. Lee, H. -I. Kim, L. Pyeon, J. Lee, T. Park, *Energy Environ. Sci.*, 2016, **9**, 2326; c) S. Jeon, U. K. Thakur, D. Lee, Y. Wenping, D. Kim, S. Lee, T. K. Ahn, H. J. Park, B. -G. Kim, *Org. Electron.*, 2016, **37**, 134; d) J. Liu, Y. Z. Wu, C. J. Qin, X. D. Yang, T. Yasuda, A. Islam, K. Zhang, W. Q. Peng, W. Chen, L. Y. Han, *Energy Environ. Sci.*, 2014, **7**, 2963; e) W. Chen, X. Bao, Q. Zhu, D. Zhu, M. Qiu, M. Sun, R. Yang, *J. Mater. Chem. C*, 2015, **3**, 10070.
- [7] a) N. J. Jeon, J. Lee, J. H. Noh, M. K. Nazeeruddin, M. Grätzel, S. I. Seok, *J. Am. Chem. Soc.*, 2013, **135**, 19087; b) D. Zhao, M. Sexton, H. -Y. Park, G. Baure , J. C. Nino, F. So, *Adv. Energy Mater.*, 2015, **5**, 1401855; c) N. J. Jeon, H. G. Lee, Y. C. Kim, J. Seo, J. H. Noh, J. Lee, S. I. Seok, *J. Am. Chem. Soc.*, 2014, **136**, 7837; d) B. Xu, E. Sheibani, P. Liu, J. Zhang, H. Tian, N. Vlachopoulos, G. Boschloo, L. Kloo, A. Hagfeldt, L. Sun, *Adv. Mater.*, 2014, **26**, 6629.
- [8] a) F. So, D. Kondakov, *Adv. Mater.*, 2010, **22**, 3762; b) Y. Shirota, M. Kinoshita, T. Noda, K. Okumoto, T. Ohara, *J. Am. Chem. Soc.*, 2000, **122**, 11021; c) L. J. Hyuk, C. H. Lee, S. C. Kim, *Material Issues of AMOLED, Organic Light Emitting Diode*, Marco Mazzeo (Ed.), InTech, 2010, DOI: 10.5772/9854.
- [9] a) J. Burschka, A. Dualeh, F. Kessler, E. Baranoff, N. L. Cevey-Ha, C. Y. Yi, M. K. Nazeeruddin, M. Grätzel, *J. Am. Chem. Soc.*, 2011, **133**, 18042; b) T. Leijtens, I. K.

- Ding, T. Giovenzana, J. T. Bloking, M. D. McGehee, A. Sellinger, *ACS Nano*, 2012, **6**, 1455. Article Online  
DOI: 10.1039/C7TA02440A
- [10] a) G. E. Eperon, V. M. Burlakov, P. Docampo, A. Goriely, H. J. Snaith, *Adv. Funct. Mater.*, 2014, **24**, 151; b) J. Liu, Y. Z. Wu, C. J. Qin, X. D. Yang, T. Yasuda, A. Islam, K. Zhang, W. Q. Peng, W. Chen, L. Y. Han, *Energy Environ. Sci.*, 2014, **7**, 2963.
- [11] Y. T. Tao, C. H. Chuen, C. W. Ko, J. W. Peng, *Chem. Mater.*, 2002, **14**, 4256; b) U. Mitschke, P. Bäuerle, *J. Mater. Chem.*, 2000, **10**, 1471.
- [12] a) Y. Xue, Y. Wu, Y. Li, *J. Power Sources*, 2017, **344**, 160; b) Z. Zhou, Y. Zhao, C. Zhang, D. Zou, Y. Chen, Z. Lin, H. Zhen, Q. Ling, *J. Mater. Chem. A*, 2017, **5**, 6613.
- [13] H. J. Park, M.-G. Kang, S. H. Ahn, L. J. Guo, *Adv. Mater.*, 2010, **22**, E247; b) H. J. Park, H. Kim, J. Y. Lee, T. Lee, L. J. Guo, *Energy Environ. Sci.*, 2013, **6**, 2203.
- [14] J. H. Park, J. Seo, S. Park, S. S. Shin, Y. C. Kim, N. J. Jeon, H.-W. Shin, T. K. Ahn, J. H. Noh, S. C. Yoon, C. S. Hwang, S. I. Seok, *Adv. Mater.*, 2015, **27**, 4013.
- [15] a) N. K. Noel, A. Abate, S. D. Stranks, E. S. Parrott, V. M. Burlakov, A. Goriely, H. J. Snaith, *ACS Nano*, 2014, **8**, 9815; b) C. Huang, W. Fu, C.-Z. Li, Z. Zhang, W. Qiu, M. Shi, P. Heremans, A. K.-Y. Jen, H. Chen, *J. Am. Chem. Soc.*, 2016, **138**, 2528; c) J. Cao, Y. M. Liu, X. Jing, J. Yin, J. Li, B. Xu, Y. Z. Tan, N. Zheng, *J. Am. Chem. Soc.*, 2015, **137**, 10914; d) D. W. deQuilettes, S. M. Vorpahl, S. D. Stranks, H. Nagaoka, G. E. Eperon, M. E. Ziffer, H. J. Snaith, D. S. Ginger, *Science*, 2015, **348**, 683; e) C. Sun, Z. Wu, H.-L. Yip, H. Zhang, X.-F. Jiang, Q. Xue, Z. Hu, Z. Hu, Y. Shen, M. Wang, F. Huang, Y. Cao, *Adv. Energy Mater.*, 2016, **6**, 1501534.
- [16] Abee, M. W.; Cox, D. F. *J. Phys. Chem. B*, 2001, **105**, 8375.

## Table of Contents entry



Triarylamine derivatives containing electron donating methoxy units provide outstanding device performance when they are adopted as dopant-free hole transporting layer in inverse type planar heterojunction perovskite solar cell (PSC). The methoxy units introduced to a conjugated scaffold critically contribute to the reduced charge recombination during PSC operation, which can be verified by time-correlated single-photon counting measurement and transient photo-voltage study.